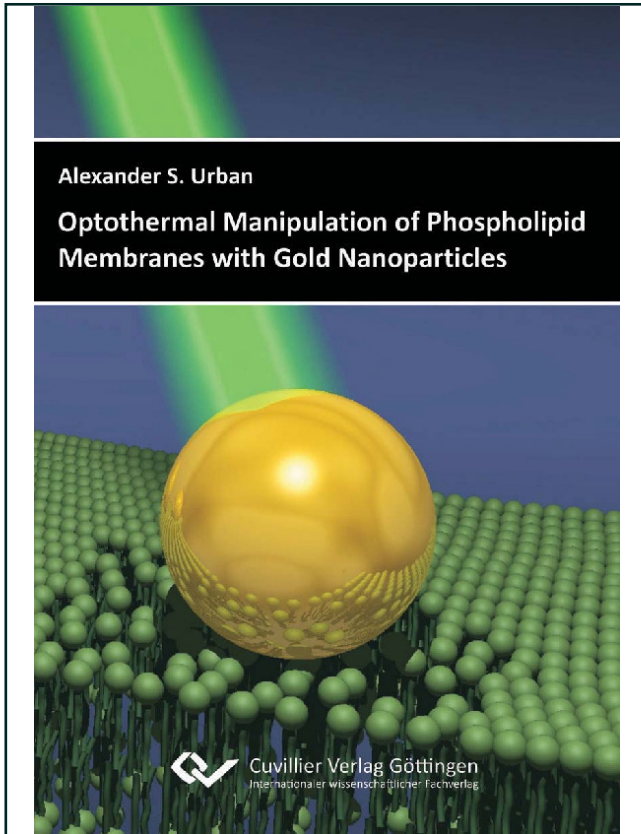




Alexander Urban (Autor)

Optothermal Manipulation of Phospholipid Membranes with Gold Nanoparticles



<https://cuvillier.de/de/shop/publications/502>

Copyright:

Cuvillier Verlag, Inhaberin Annette Jentsch-Cuvillier, Nonnenstieg 8, 37075 Göttingen, Germany

Telefon: +49 (0)551 54724-0, E-Mail: info@cuvillier.de, Website: <https://cuvillier.de>

2.1 Optical and Thermal Properties of Gold Nanoparticles

The Romans were known for their many inventions and were in fact among the first to use metallic nanoparticles, although unknowingly³⁷. The *Lycurgus Cup*, depicting the Greek king Lycurgus being dragged to the underworld, is one of the first examples of how gold nanoparticles, typically 5 – 60 nm in size, can be used to colour glass in an extraordinary way (Figure 2.1). In ordinary daylight the cup has a predominantly green color; however it appears red when illuminated from the inside. This amazing effect results from the characteristic properties of metallic nanoparticles and the way they interact with light.

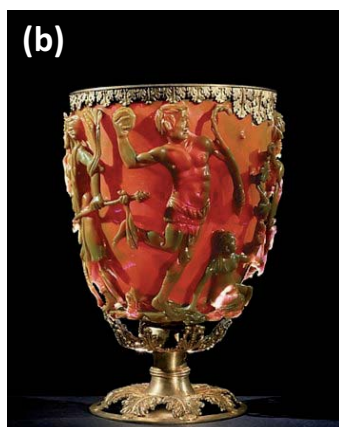
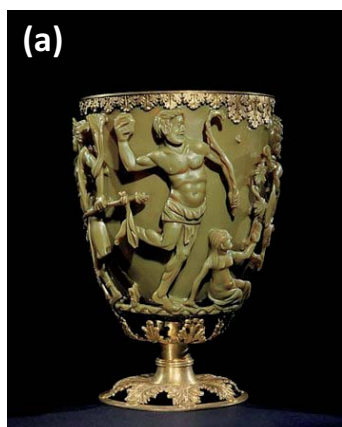


Figure 2.1 | The Lycurgus Cup is an excellent example of the optical properties of gold. (a) When illuminated from the outside, the gold nanoparticles inside the glass cup scatter the light, making the cup appear green. (b) However, when a light is placed inside the cup, the absorption of the gold nanoparticles changes the cup's apparent color to red.

2.1.1 Optical Properties

The noble metals copper (Cu), silver (Ag) and gold (Au) are all elements belonging to the 11th group of the periodic table. The electron configurations of these elements are exceptions to the *Madelung rule*, which describes the filling order of the atomic subshells. All of these elements have completely filled d-subshells (respectively 3d, 4d and 5d); their core electrons are in the so called inert gas configuration. Their metallic properties result from the lone valence electron in the half-filled s-subshells (4s, 5s and 6s respectively). The band structure of gold displays five comparatively flat d-bands, lying 1 – 3 eV below the *Fermi energy*, E_F , in which the ten d-electrons are located (Figure 2.2). The lone s-electron forms an sp-hybridised band, which is

filled up to E_F . Electrons in this band can move quasi-free due to the near parabolic form of the band. This band structure defines the characteristic properties of these metals, such as their thermal and electrical conductivity.

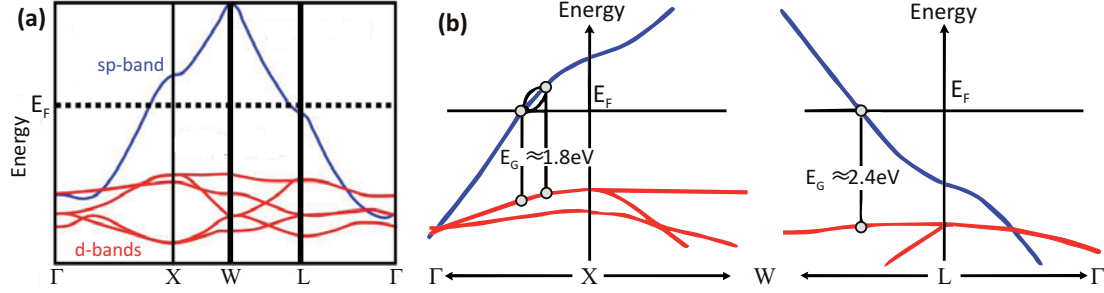


Figure 2.2 | The band structure of gold. (a) The sp-band has a nearly parabolic form leading to quasi-free electrons. (b) Interband transitions in gold occur near the X- and L- points in the first Brillouin zone. (Taken from^{38,39})

2.1.1.1 Dielectric Properties of Gold

The electrons in this band can be seen as free electrons because of the near-parabolic sp-band of gold. An accurate description is given by the *Drude-Sommerfeld theory*⁴⁰. This model depicts the electrons as a gas of independent, quasi-free point-shaped particles that are accelerated by an external electric field and slowed down after a mean free time, $\tau = \Gamma^{-1}$, through collisions with metal ions (for gold⁴¹: $\tau = 30$ fs at 273 K). Scattering processes are the reason that the electrons are called *quasi-free* and not *free*. The Drude-Sommerfeld model determines the response function or *dielectric function*, $\varepsilon(\omega)$, of a macroscopic metal by calculating the behavior of a single conduction electron and multiplying this behavior by the number of electrons present. This is only valid when assuming the independence of the single electrons, as stated above. The equation of motion for an electron of mass, m_e , and charge, e , in an external electric field $\vec{E} = \vec{E}_0 e^{-i\omega t}$ is given by:

$$m_e \frac{\partial^2 \vec{r}}{\partial t^2} + m_e \Gamma \frac{\partial \vec{r}}{\partial t} = e \vec{E}_0 e^{-i\omega t} \quad (2.1)$$

with the damping constant, Γ . This differential equation is valid for a model system without eigenfrequencies for $\omega > 0$ and only takes into account the effect on

the conduction band electrons. In order to incorporate bound electrons, a linear restoring force, determining the eigenfrequency of the oscillating electrons, would have to be added to the equation. Solving equation 2.1 leads to the dipole moment of a single electron, $\vec{p} = e\vec{r}_0$, and the polarization, $\vec{P} = n\vec{p}$, with the number of electrons per unit volume, n . The dielectric function, $\varepsilon(\omega) = \varepsilon_1(\omega) + i\varepsilon_2(\omega)$, is related to the polarization via the definition $\varepsilon = 1 + P/(\varepsilon_0 E)$ and to the complex refractive index via $n + ik = \sqrt{\varepsilon}$. This leads to the dielectric function of a system of n free electrons per unit volume:

$$\varepsilon(\omega) = 1 - \frac{\omega_p^2}{\omega^2 + i\Gamma\omega} = 1 - \frac{\omega_p^2}{\omega^2 + \Gamma^2} + i\frac{\omega_p^2\Gamma}{\omega(\omega^2 + \Gamma^2)} \quad (2.2)$$

which is only determined by the *plasma frequency*, $\omega_p = \sqrt{ne^2/\varepsilon_0 m^*}$, and the relaxation constant, Γ . This can be determined from the electron mean free path, l by $\Gamma = v_F/l$, where v_F is the *Fermi velocity*. If the damping is much smaller than the frequency, the real and imaginary parts of the dielectric function can be written as:

$$\varepsilon_1(\omega) \approx 1 - \frac{\omega_p^2}{\omega^2}, \quad \varepsilon_2(\omega) \approx 1 - \frac{\omega_p^2}{\omega^3}\Gamma. \quad (2.3)$$

This equation shows that for $\varepsilon_1(\omega) = 0$ the frequency, ω , equals the plasma frequency, ω_p . The dielectric function, $\varepsilon(\omega)$, is commonly expressed in terms of the electric susceptibility, χ . Then equation 2.2 becomes:

$$\varepsilon(\omega) = 1 + \chi_{DS}(\omega) \quad (2.4)$$

where χ_{DS} is the free-electron Drude-Sommerfeld susceptibility. Electrons in a real metallic lattice are only quasi-free due to the lattice periodicity. The coupling of the free electrons to the ion core is taken into consideration by replacing the electron mass, m_e , with an effective electron mass, m^* , effectively altering ω_p .

Not only the conduction band electrons but also electrons from deeper levels contribute to the dielectric function. Direct excitations of electrons from the 5d-band to vacant states above E_F in the 6sp-band can take place near the X- and L- points

in the first Brillouin zone (Figure 2.2a). These optical excitations exist both in gold nanoparticles as well as in bulk gold and begin at the inter-band gap $E = 1.7 \text{ eV}$ ^{39,42} (Figure 2.2b). However, the oscillator strength of this transition near the X-point is so low that in measurements of the optical density of gold colloidal solutions this transition can not be seen. Instead, the transition near the L-Point with $E = 2.38 \text{ eV}$ becomes visible as a constantly increasing background, independent of nanoparticle size (Figure 2.3). This effect leads to an additional term in the susceptibility and equation 2.2 becomes:

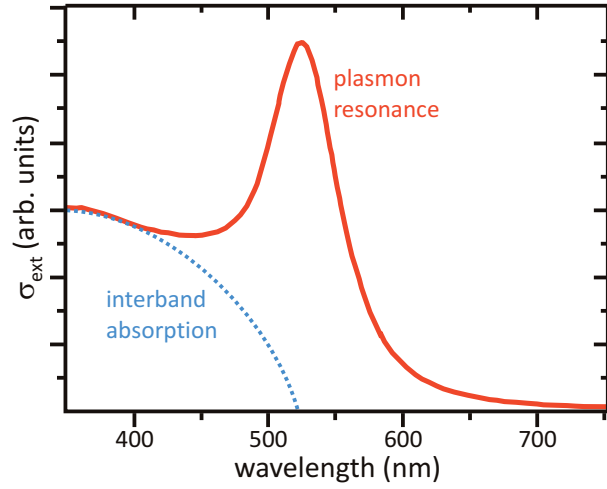


Figure 2.3 | Extinction spectrum of a colloidal suspension of 40 nm gold nanoparticles. The plasmon resonance is centered at 528 nm. The contribution of intraband excitations is clearly seen for wavelengths below 520 nm.

$$\varepsilon(\omega) = 1 + \chi_{DS} + \chi_{IB} \quad (2.5)$$

with the interband susceptibility, $\chi_{IB} = \chi_{IB,1} + i\chi_{IB,2}$. The imaginary part describes the direct energy dissipation and is thus only large for frequencies at which interband transitions occur. The real part however is also important for smaller frequencies⁴⁰.

The dielectric functions of nanoparticles with a diameter that is larger than approximately 10 nm are size-independent and become like those of bulk-gold. Smaller nanoparticles are considerably smaller than the electron mean free path, $l = v_F\tau = 42 \text{ nm}$. In these, the electrons cannot cover this distance without scattering at the nanoparticle surface. This reduced mean free path has been confirmed experimentally^{43,44} and causes the homogeneous linewidth of the plasmon resonance to greatly increase for these nanoparticles. As stated before, bound electrons (e.g. the d-band electrons) have not been accounted for yet as the Drude-

Sommerfield model only considers free-electrons⁴⁵. Modeling these electrons is extremely difficult⁴⁶. Normally, instead of using corrected values for the dielectric function, experimental ones are used. The main source for these values comes from the work of Johnson and Christie, who measured the optical properties of bulk gold in 1972⁴⁷. In all calculations conducted within this thesis these values were used. This is valid, because all of the nanoparticles used were larger than 10 nm.

Due to the energy dissipation of electromagnetic waves impinging on a metal surface, these only have a limited penetration depth which can be calculated from the optical functions. Assuming a plane wave incident in the z-direction and expressing the wave vector, \vec{k} , as $|\vec{k}| = (\omega/c)(n + ik)$, the electric field within the metal can be expressed as:

$$\vec{E}(\vec{r}, t) = \vec{E}_0(\vec{r}, t)e^{i\omega(zn/c-t)}e^{-z/d} \quad (2.6)$$

with the attenuation of the field determined by the *skin depth*, $d = \frac{c}{\omega k} = \frac{\lambda}{2\pi k}$, and the optical function, $n + ik = \sqrt{\varepsilon_1 + i\varepsilon_2}$. The skin depth is wavelength dependent and assumes values for gold between 31 nm at 620 nm incident wavelength and 37 nm at 413 nm.

2.1.1.2 Electrodynamic Calculations of Spherical Particles (Mie Theory)

In order to calculate the response of a metal nanoparticle to an external electromagnetic field, one must solve Maxwell's equations. Fortunately, an analytical solution already exists. Danish physicist Ludvik Lorenz first published this in 1890, however only in Danish. Later, Gustav Mie "rediscovered" it in 1908, wherefore it is generally known as *Mie-Theory*. The theory is valid for all nanoparticle sizes and optical wavelengths in contrast to Rayleigh's scattering theory, which is limited to nanoparticles much smaller than the wavelength of the incident radiation. In fact, Rayleigh scattering is a first-order approximation of Mie-Theory.

In his solution of the Maxwell equations, Mie describes the interaction between a plane wave and uncharged homogeneous particles. This allows the precise calculation of the electromagnetic fields within and surrounding the particle. The

spherically symmetrical geometry suggests a multipole expansion of the fields. The resulting surface harmonics enable the calculation of the extinction, scattering and absorption cross-sections of the particles:

$$\sigma_{ext} = \frac{2\pi}{|k|^2} \sum_{n=1}^{\infty} (2n+1) \text{Re}[a_n + b_n] \quad (2.7)$$

$$\sigma_{sca} = \frac{2\pi}{|k|^2} \sum_{n=1}^{\infty} (2n+1) [|a_n|^2 + |b_n|^2] \quad (2.8)$$

$$\sigma_{abs} = \sigma_{ext} - \sigma_{sca} \quad (2.9)$$

with the Mie-coefficients from the multipole expansion, a_n and b_n , the multipole order, n , ($n = 1$ corresponds to the dipole mode) and the wave vector of the incident electromagnetic wave, \vec{k} . "Re" signifies that only the real part of the bracket is taken. The Mie-coefficients are:

$$a_n = \frac{m \psi_n(mx) \psi'_n(x) - \psi_n(x) \psi'_n(mx)}{m \psi_n(mx) \eta'_n(x) - \eta_n(x) \psi'_n(mx)} \quad (2.10)$$

$$b_n = \frac{\psi_n(mx) \psi'_n(x) - m \psi_n(x) \psi'_n(mx)}{\psi_n(mx) \eta'_n(x) - m \eta_n(x) \psi'_n(mx)} \quad (2.11)$$

with the Riccarti-Bessel functions, ψ_n and η_n , the ratio of the complex refractive indices of the particle and the surrounding medium, $m = n_{part}/n_{medium} = \sqrt{\epsilon_r}$, and the ratio of the particle radius, r , to the wavelength of the scattered light, λ , being $x = 2\pi r/\lambda$. In this work, calculations of the cross sections of gold nanoparticles were carried out with the program MQMie⁴⁸. With this program it is also possible to account for core-shell particles or uncharged surface ligand molecules.

2.1.1.3 Electrostatic and Quasi-Static Modeling

Mie theory is excellent for calculating scattering and absorption by spheres because it is an exact theory. However, calculating the exact results for geometries more complex than spheres can be extremely time consuming and is not always necessary. Furthermore, Mie theory is not always the best choice when one wants to acquire some intuitive feeling for how a sphere of a given size and optical properties absorbs

and scatters light. This is facilitated by applying electrostatics. Here the electromagnetic field imposing on the metal nanoparticles is both spatially and temporally constant. Considering the boundary-conditions that the tangential components of the electric and magnetic fields must be continuous at the particle surface⁴⁹, one obtains the electric field inside the nanoparticle:

$$E_i = E_0 \frac{3\varepsilon_m}{\varepsilon + 2\varepsilon_m} \quad (2.12)$$

with the dielectric constant of the surrounding medium, ε_m . The internal field directly supplies the static polarizability of the sphere, $\alpha = p/\varepsilon_m E_0$:

$$\alpha = 4\pi\varepsilon_0 R^3 \frac{\varepsilon - \varepsilon_m}{\varepsilon + 2\varepsilon_m} \quad (2.13)$$

This electrostatic approach can be extended even further to the *quasi-static regime* in which the electromagnetic field is still spatially constant but now has a time dependence ($\vec{E} \rightarrow \vec{E}(t)$). To account for this, ε and ε_m in equations 2.12 and 2.13 must be replaced by their frequency dependent functions, $\varepsilon(\omega)$ and $\varepsilon_m(\omega)$; excitations induced by the magnetic field are neglected. Resonances then occur for both the internal electric field and the polarizability, when the denominator becomes minimal:

$$[\varepsilon_1(\omega) + 2\varepsilon_m]^2 + [\varepsilon_2(\omega)]^2 \rightarrow \text{minimal} \quad (2.14)$$

Thus a negative ε_1 is necessary, or in the special case of a small $\varepsilon_2 \ll 1$, or a small frequency dependency $\partial\varepsilon_2/\partial\omega$, the resonance condition becomes:

$$\varepsilon_1 = -2\varepsilon_m \quad (2.15)$$

This then leads to the position of the resonance using the approximative equation 2.3 for free-electron metals and $\varepsilon_m = 1$:

$$\omega_1 = \frac{\omega_p}{\sqrt{3}} \quad (2.16)$$

What has been done here in basic terms is to use a simple oscillator model to calculate the *Drude eigenfrequency* for free electron nanoparticles. In this model

the free electrons from the sp-band are displaced by an incoming electric field, E_{in} , (Figure 2.4). The Coulomb interaction between the displaced electrons and the positive charges left behind by the stationary atomic cores serves as a restoring force with the surface polarization supplying the majority of this force. The electrons oscillate collectively and the oscillation is allocated with a bosonic quasiparticle, the *surface plasmon*. Its frequency, ω_1 , was derived in equation 2.16. This theory can easily be extended to metal spheroids or ellipsoids, in which case the eigenfrequency, ω_1 , depends on the spatial orientation, resulting in a separate eigenfrequency for each independent spatial direction.

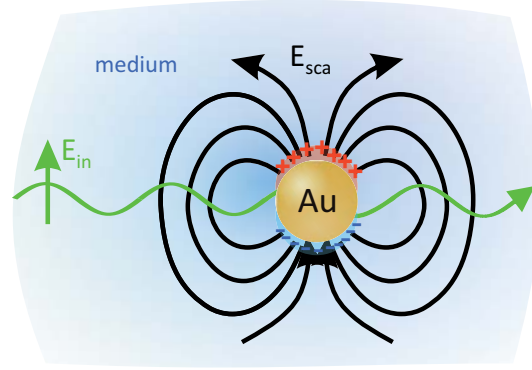


Figure 2.4 | Formation of a surface plasmon in a gold nanoparticle. An electromagnetic wave penetrates the nanoparticle completely and induces the conduction band electrons to oscillate. This induced Hertz-dipole produces radiation.

The resonance wavelengths or frequencies of plasma resonances of metal nanoparticles can be easily analyzed in the quasi-static regime. As stated previously, this is only valid for very small nanoparticles ($2r \ll \lambda$). In this case, phase retardation and effects of higher multipoles are neglected and the Mie formula is drastically simplified. Using $k = \omega/c$ as the lowest order term, equation 2.7 becomes^{40,50}:

$$\sigma_{ext}(\omega) = 9 \frac{\omega}{c} \varepsilon_m^{3/2} V_{np} \frac{\varepsilon_2}{(\varepsilon_1(\omega) + 2\varepsilon_m)^2 + (\varepsilon_2(\omega))^2} \quad (2.17)$$

with the nanoparticle volume, $V_{np} = 4/3\pi r^3$, the dielectric function of the medium, ε_m , and the complex dielectric function of the nanoparticle, $\varepsilon_{np}(\omega) = \varepsilon_1(\omega) + i\varepsilon_2(\omega)$. This extinction cross section describes only dipolar absorption. The scattering cross section (equation 2.8), proportional to R^6 and higher multipolar contributions ($\sigma_{ext,quadrupol} \propto R^5$, $\sigma_{sca,quadrupol} \propto R^{10}$) are highly suppressed at $2r \ll \lambda$. The resonance condition $\varepsilon_1(\omega) = -2\varepsilon_m$ is well met by alkali metals, but not by free electron metals such as gold. Here, where $\omega \gg \Gamma$, the shape and position of the

resonance can be estimated by inserting equation 2.3 into equation 2.17. This results in an extinction coefficient of:

$$\sigma_{ext}(\omega) = \sigma_0 \frac{1}{(\omega - \omega_1)^2 + (\Gamma/2)^2} \quad (2.18)$$

The shape of the extinction is thus Lorentzian in the vicinity of the resonance, whose position can be calculated directly from the plasma frequency:

$$\omega_1 = \frac{\omega_p}{\sqrt{1 + 2\varepsilon_m}} \quad (2.19)$$

2.1.1.4 Damping Mechanisms of the Surface Plasmon

The damping in the system is due to scattering of the electrons at other electrons, phonons, lattice defects, the particle surface, etc. such that the damping constant, Γ , results from the average of the collision frequencies of the electrons. For independent collision processes, i , the *Matheisen rule* applies and Γ is the result of the summation of all collisional frequencies:

$$\Gamma = \tau^{-1} = \sum_i \tau_i^{-1} = \tau_{e-e}^{-1} + \tau_{e-phonon}^{-1} + \tau_{impurities}^{-1} + \dots \quad (2.20)$$

Experimentally, Γ is determined by measuring the macroscopically available electrical conductivity, ρ_{el} , and inserting this into $\Gamma = \rho_{el} n e^2 / m^*$.

As stated before, the collective oscillation of the sp-electrons can be described as a bosonic quasiparticle, the plasmon. An excited plasmon can decay through a multitude of channels. These are divided into two main groups, radiative and non-radiative decay processes (Figure 2.5). The radiative decay occurs via emission of photons, which can be seen in the far-field as scattered light. This is described in the classical picture of a Hertz dipole via the periodical acceleration of electrons away from their equilibrium positions. This leads to the emission of energy via radiation by the nanoparticle. According to the Abraham-Lorentz equations of motion, which are extensions of the Drude-Sommerfeld theory, the radiative decay rate in a nanoparticle, R_{rad} , is size-dependent⁵¹:

2.1. Optical and Thermal Properties of Gold Nanoparticles

$$R_{rad} \propto V \propto r^3 \quad (2.21)$$

Thus, the probability that the plasmon decays radiatively is directly proportional to the nanoparticle volume, i.e. to the cube of the nanoparticle radius. The plasmon resonance becomes very clear in the scattering spectrum of gold nanoparticles. Even 40 nm nanoparticles can be seen easily in a dark field microscope^{52,53}.

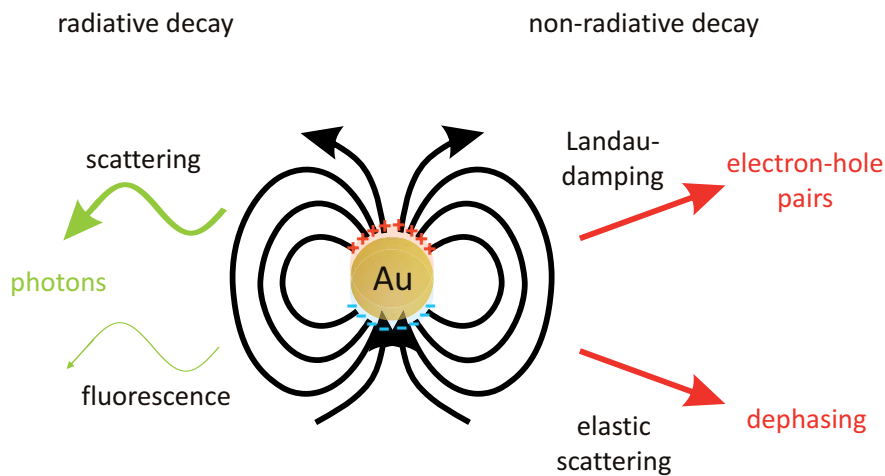


Figure 2.5 | Surface plasmons can decay either via radiative (left) or non-radiative processes (right). The fluorescence emission of gold is negligible, however¹⁹.

The non-radiative decay of the surface plasmon leads to the nanoparticle absorbing the incident light, which is converted efficiently into heat. This process is essential for the work done here and will be described in more detail in section 2.1.2. The most important damping mechanism for the optothermal properties of gold nanoparticles is Landau damping. Here the plasmon decays non-radiatively by creating electron-hole pairs. One must distinguish between excitation of electron-hole pairs inside the *sp*-band (*intraband* excitation) and the excitation of electrons from the energetically deeper *d*-band into the *sp*-band (*interband* excitation). A further decay channel is the elastic scattering of the oscillating electrons. These can scatter from each other, from phonons, lattice defects, impurities or from the particle surface and thus come out of synchrony with each other. This leads to a dephasing of the electrons.